energies

MDPI

Article

A Simple and Accurate Energy-Detector-Based Transient Waveform Detection for Smart Grids: Real-World Field Data Performance †

Ali Riza Ekti [1,*], Aaron Wilson [1], Joseph Olatt [1], John Holliman II [1], Serhan Yarkan [2] and Peter Fuhr [1]

[1] Electrification and Energy Infrastructures Division, Oak Ridge National Laboratory, Oak Ridge, TN 37830, USA
[2] Department of Electrical and Electronic Engineering, Istanbul Ticaret University, 34469 Istanbul, Turkey
* Correspondence: ektia@ornl.gov

Abstract: Integration of distributed energy sources, advanced meshed operation, sensors, automation, and communication networks all contribute to autonomous operations and decision-making processes utilized in the grid. Therefore, smart grid systems require sophisticated supporting structures. Furthermore, rapid detection and identification of disturbances and transients are a necessary first step towards situationally aware smart grid systems. This way, high-level monitoring is achieved and the entire system kept operational. Even though smart grid systems are unavoidably sophisticated, low-complexity algorithms need to be developed for real-time sensing on the edge and online applications to alert stakeholders in the event of an anomaly. In this study, the simplest form of anomaly detection mechanism in the absence of any a priori knowledge, namely, the *energy detector (also known as radiometer in the field of wireless communications and signal processing)*, is investigated as a triggering mechanism, which may include automated alerts and notifications for grid anomalies. In contrast to the mainstream literature, it does not rely on transform domain tools; therefore, utmost design and implementation simplicity are attained. Performance results of the proposed energy detector algorithm are validated by real power system data obtained from the DOE/EPRI National Database of power system events and the Grid Signature Library.

Keywords: transient and anomaly detection; energy detector; grid signature library; arcing; wildfire; smart grid

Citation: Ekti, A.R.; Wilson, A.; Olatt, J.; Holliman, J., II; Yarkan, S.; Fuhr, P. A Simple and Accurate Energy-Detector-Based Transient Waveform Detection for Smart Grids: Real-World Field Data Performance. *Energies* **2022**, *15*, 8367. https://doi.org/10.3390/en15228367

Academic Editor: Hongjun Gao

Received: 13 September 2022
Accepted: 7 November 2022
Published: 9 November 2022

1. Introduction

The power system is indispensable to contemporary human civilization. Nearly every device, system, and service is directly or indirectly connected to the grid. Service interruptions have serious consequences, including fires, explosions, disconnection of critical medical equipment, interruption of communications and transportation, water contamination, and more. Therefore, advanced metering, real-time monitoring, and alerting systems should always accompany the power system network, which enables the smart grid [1,2]. The smart grid is expected to enhance reliability, security, and efficiency of the power network; dynamically optimize the grid operations and its resources; and be fully aware of cyber-security concepts such as proactive cyber-defense.

The complexity of smart grid systems with more distributed energy sources leads to enriched transient disturbances and insufficient protection. Transient detection, classification, and localization is crucial to improve the overall performance and to eliminate

any interruptions for smart grid systems [3,4]. One prominent example of such a critical problem is high impedance faults such as "arcing". Over the past five years, power line malfunctions have sparked wildfires such as Dixie, Thomas, Camp, Red-wood Valley, Atlas, and Nuns, leading to 106 fatalities and enormous economic losses [5]. While fires due to "equipment failure" or "electrical power" constitute a relatively modest 20% of the total, the environmental impact of these events includes an outsized 1.5 M acres burned [5]. Evidently, accurate and reliable detection of transients with low-complexity methods should be the first priority to protect critical infrastructures and prevent catastrophic events.

One of the most important characteristics of power grid systems is the energy-carrying sinusoid whose frequency is strictly controlled by the grid. However, this fundamental frequency is subject to oscillations caused by mismatches between generation and load. This poses the following problems: (i) In the case where the frequency is assumed to be fixed throughout the operation, it implies that any actual deviation from the assumed fixed value will degrade the estimation accuracy. Furthermore, in the case where the deviation is not compensated for, the upcoming estimations will suffer from previous estimation errors propagating into future stages. (ii) If this frequency is not assumed to be fixed, then the estimation method mandates the frequency estimation procedure to be applied at every stage in order to maintain the desired accuracy. Any detection system that relies on frequency, whether fixed or not fixed, will compromise between estimation accuracy and computational complexity. Therefore, in this study, we propose a low-cost energy detector (also known as a radiometer in the field of wireless communications and signal processing) approach for accurate and reliable transient detection.

1.1. Related Work

Various time–frequency algorithms are applied to detect and identify the power grid anomalies under different categories and classifications [6]. However, one of the most prominent ways of approaching the methods present in the literature is to check whether the methods proposed include frequency domain tools and/or joint transform domain analysis. From this perspective, in the literature, there are studies that strive to increase their efficiencies by jointly analyzing frequency and temporal domain characteristics. For instance, in [7], a short-term Fourier transform (STFT) approach is proposed to detect and identify the anomalies present in the grid signals. Considering the fact that STFT is a computationally expensive operation, a dictionary might be a viable option in terms of execution time; however, preparation, construction, and update of the dictionary itself still remain to be detailed since they inherently affect the performance of the proposed method. Another joint time–frequency based approach is based on discrete wavelet transform (DWT) [8]. It is clear that even though DWT performs outstandingly, especially in anomalies that include abrupt changes in time, it is by definition based on a set of computationally intensive operations. Having said that, one should state that superior performance is directly related to the appropriate kernel selection, which is driven by the nature of the problem of interest. Rather than proposing a single method and looking at the problem from a single perspective, hybrid methods are proposed in the literature as well in order to overcome the shortcomings of each individual method. For example, in [9], a combiner is brought up to improve the performance of detection of several different types of anomalies. Nevertheless, it is not very well established how different combiner approaches perform as well as how temporally superposed anomalies behave in different scenarios. Another umbrella method that could be found in the literature is based on decision tree approach [10] such that prominent statistics are first obtained to decide which branch of the tree is selected. Based on the initial results, further classification is applied with decision tree.

In contrast to sophisticated transform-domain oriented studies, in the literature, there exist several studies of radiometers modified for anomaly detection in power grid signals as well. For instance, a root mean square (RMS) energy filter approach is proposed in [11]; however, the method proposed in [11] suffers from the following two issues: First, the

threshold selection mechanism is fortified with frequency-domain processing, which is a computationally intensive routine. Second, the temporal resolutions of the filters at bandpass and low-pass regions are relatively low, which are inappropriate in detecting and/or identifying extremely fast, impulsive-behavior transients. Another frequency-domain benefiting method is given in [12], which takes advantage of a stringent, constant, frequency-domain-dependent value for test statistic. Clearly, in case any drift takes place in the frequency-domain-dependent parameter, the anomaly detection procedure ends up having timing offsets. Furthermore, critical computation steps of the proposed method (Equations (3) and (4) in [12]) rely inherently on some sort of frequency estimation or fixed frequency assumption. Evidently, such an estimation or assumption brings about an extra layer of complexity in the proposed method.

In contrast to both [11,12], in [13], a highly sophisticated version of the radiometer is indirectly employed for anomaly detection. Besides the computational burden of the method proposed in [13], it also suffers from the presence of differential operator, which is very well known to be problematic in both accurately obtaining the amplitude of full-scale, monochromatic signals and exacerbating the impact of broad- or wide-band noise that is inherently present in any system. Furthermore, the method in [11–13] benefits also from frequency estimation with certain tolerance. Therefore, it also comes at the expense of escalated sophistication in design. Even though not directly operating on direct measurement data, in [14], the traditional radiometer operating on acoustic signals is reinforced firstly by a pre-filtering block and secondly by a set of higher-order statistical parameters. There are many other radiometer-derivative methods employed in the literature for anomaly detection, such as that in [15]. Although those methods might outperform the traditional radiometer to some extent under certain circumstances, all of the derived methods present in the literature come at the expense of sophisticated design and/or implementation as compared with the pure, traditional radiometer.

1.2. Contributions

The current work extends previous studies by employing a pure, traditional, and plain radiometer method without any modifications and/or extensions. In this regard, the contributions of this study are three-fold: (i) It is demonstrated theoretically that detection of various types of anomalies could be achieved with a radiometer method without necessitating any frequency or period estimation. (ii) The traditional radiometer could be adapted with a single parameter to human intervention scenarios, which is frequently encountered/desired in real-world field operations. (iii) The proposed method is tested and validated with real-world field data including both short- and long-living transients as well as slow-envelope-changing anomalies with various peak-to-average power ratio (PAPR) behaviors such as in arcing faults.

Based on the discussions carried out in both Sections 1.1 and 1.2, a general comparison between the prominent studies in the literature as well as the proposed method is given in Table 1. Note that the proposed method stands out from both the perspective of implementation difficulties and eliminating the a priori use of information and/or transform domain tools or methods.

1.3. Organization

The remainder of this study is organized as follows. We present the signal model and energy detector approaches in Section 2, a detailed explanation of the proposed energy detector approach in Section 3, numerical results in Section 4, a runtime analysis in Section 5, and concluding remarks in Section 6.

Table 1. Comparison between prominent studies in the literature on several aspects.

Publications	Complexity	A Priori Information	Use of Transform Domain	Implementation Difficulty
[6]	High	Yes	Yes	High
[7]	Medium	Yes	Yes	Medium
[8]	High	Yes	Yes	High
[9]	High	No	Yes	High
[10]	High	No	Yes	High
[11]	Medium	Yes	Yes	Medium
[12]	Medium	No	Yes	Medium
[13]	Medium	No	No	Medium
[14]	Medium	No	Yes	Medium
[15]	Medium	No	No	Medium
The proposed method	Medium	No	No	Low

2. Signal Model

An idealized representation of a voltage or current signal measurement is

$$s(t) = A\cos(2\pi f_0 t + \theta), \tag{1}$$

where A denotes the amplitude, f_0 is the fundamental frequency (50 or 60 Hz depending on location), and θ its phase. These parameters are assumed to be constants of the observation period.

A generic smart grid measurement system uses an analog-to-digital converter (ADC) satisfying the Nyquist criterion to transform the ideal signal into a discrete-time signal.

$$s[n] = A\cos\left(2\pi f_0 \frac{n}{Fs} + \theta\right) \tag{2}$$

where n is the index of the sampled signal and F_s denotes the sampling frequency adopted by the ADC. Considering that the signal that is sampled is contaminated with certain disturbances and/or perturbations, and $h[n]$ represents an ideal transmission line with no significant delay, a more realistic discrete-time signal model would be

$$r[n] = h * s[n] + w[n] + q[n]p_{T_q}[n - N_p] \tag{3}$$

where $r[n]$ is the "more realistic" signal captured by ADC; h denotes the gain of the ideal transmission line; $*$ denotes the discrete-time convolution operation; $w[n]$ is the additive ambient noise; $q[n] \neq 0$ is the random process characterizing the anomaly of interest; $p_{T_q}[n]$ denotes the windowing function that captures the duration of the short-term transient; and N_p stands for the delay that determines the temporal location of the contaminating random process. Besides $w[n]$, there are certain aspects regarding the disturbance $q[n]p_{T_q}[n - N_p]$. First and foremost, it is expected that $q[n]$ is relatively short, which is controlled by the parameter T_q affiliated with $p_{T_q}[\cdot]$. So, in case the presence of $q[n]$ is desired to be estimated, T_q should be detected. Moreover, it is expected that $q[n]$ is relatively broadband and probably a stationary random process in the wide-sense that is impinged on $s[n]$ whose R-th realization could be given by

$$q_R[n] = a_0^R + \sum_{k=1}^{M_R}\left(a_k^R \cos\frac{k\pi n}{L_R} + b_k^R \sin\frac{k\pi n}{L_R}\right) \tag{4}$$

where M_R is the number of harmonics contributing to the process; a_k^R and b_k^R are the k-th real-valued coefficients of the k-th harmonic; and L_R denotes the control parameter of the fundamental normalized period belonging to R-th realization.

In this regard, the anomaly detection problem utilizing the energy detector can be reduced to the traditional hypothesis test:

$$H_0 : p_{T_q}[n] = 0$$
$$H_1 : p_{T_q}[n] \neq 0. \tag{5}$$

2.1. Energy Detector

In wireless communications, the traditional energy detector is based on the concept of a simple, first-order, non-coherent receiver. More importantly, it is the "optimum" detector when there is no a priori knowledge about the received signal. Simplicity in design provides efficient implementation and tractable statistical analysis. The traditional energy detector consists of a full-wave rectification and a low-pass filtering operation at baseband. From the perspective of discrete-time analysis, the energy detector can simply be expressed as [16]

$$\psi[n] = \sum_{i=0}^{N-1} |r[n-i]|^2 \tag{6}$$

where ψ denotes the decision statistic, N is the number of samples taken into consideration, and $\cdot[n]$ denotes the n-th discrete-time sample. There are several points regarding Equation (6). It is worth mentioning that selecting a large N brings about the following two issues: on one hand, it gives rise to better resolution in terms of obtaining sufficient statistics; on the other hand, it implies that acquiring $\psi[n]$ lags behind due to buffering and processing delays. At this point, several critical statistical properties of $\psi[n]$ could be revised. The energy detector output for hypothesis H_0 corresponds to the case where $p_{T_q}[n] = 0$.

The energy detector output probability density function (PDF) under the null hypothesis H_0 is expressed as [17]

$$f_{\chi^2_N}(x) = \frac{x^{N/2-1}e^{-\frac{x}{2}}}{2^{N/2}\Gamma(N/2)} \tag{7}$$

where $\Gamma(\cdot)$ denotes the gamma function. In parallel, the PDF under H_1 hypothesis is expressed as [17]

$$f_{\chi^2_{N,m}}(x) = \frac{1}{2}\left(\frac{x}{m}\right)^{N/4-\frac{1}{2}} e^{-\frac{m+x}{2}} J_{N/2-1}(\sqrt{mx}) \tag{8}$$

where the m parameter represents the centrality behavior of Chi-square, which is a function of the design of the energy detector, and $J_k(\cdot)$ denotes the k-th order modified Bessel function of the first kind. Moving from both $f_{\chi^2_N}(x)$ and $f_{\chi^2_{N,m}}(x)$, receiver operating characteristic (ROC) (The area under the ROC curve shows how well a binary classifier can diagnose a problem when the discrimination threshold is changed.) could theoretically be obtained by analyzing $\Pr(\chi^2_N > \lambda H_1)$ and $\Pr\left(\chi^2_{N,m} > \lambda H_0\right)$, which refer to the probability of detection and the probability of false alarm, respectively. Here, $\Pr(\chi^2_N > \lambda H_1)$ is $Q_g(\sqrt{2\gamma}, \sqrt{\lambda})$, where λ represents the decision threshold, $Q_g(\cdot)$ is the generalized Marcum-Q function, and γ is the instantaneous signal-to-noise ratio (SNR). For H_1, the contribution from a pulse with $p_{T_q}[n] \neq 0$ would change the non-centrality of $f_{\chi^2_{N,m}}(x)$. Hence, threshold selection becomes critical for the decision statistics.

2.2. Threshold Selection Mechanism

Depending on the architecture of the proposed method, the threshold γ could be adjusted by an operator. Such a strategy, though easy to implement, has major drawbacks. Operator bias in establishing thresholds not only makes it difficult to resolve problems in the architecture but also differs from one operator to another. On the other hand, operator intervention fosters design simplicity since the burden is on the operator rather than the algorithm. Threshold selection by an experienced operator is often best. It represents a compromise between the unacceptable performance degradation due to use of a constant threshold value and the undesirable design complexity of an adaptive thresholding scheme.

Optimal Threshold with Maximum Likelihood Estimation

Note that once the fundamental parameters of the signal, whether voltage or current, in Equation (2) are considered, one could state that (In Equation (9)), $\hat{(\cdot)}$ values are to be estimated by utilizing maximum likelihood estimation (MLE).)

$$\hat{s}[n] = \hat{A}\cos\left(2\pi\hat{f}_c\frac{n}{Fs} + \hat{\Theta}\right) \tag{9}$$

Here, especially in high SNR regimes, as well as considering the channel model given in Equation (2), $\hat{A} \approxeq h \times A$. Therefore,

$$h \times \hat{s}[n] = A\cos\left(2\pi\hat{f}_c\frac{n}{Fs} + \hat{\Theta}\right) \tag{10}$$

The residuals, which comprise the error vector, are

$$e[n] = r[n] - A\cos\left(2\pi\hat{f}_c\frac{n}{Fs} + \hat{\Theta}\right) \tag{11}$$

which could be approximated under high SNR regime asymptotically by

$$e[n] \approxeq w[n] + q[n]p_{T_q}[n - N_p] + \epsilon_N \tag{12}$$

where $\epsilon_N \to 0$ as $N \to \infty$.

After some mathematical manipulations, the MLE of $\mathbf{U}$, denoted $\hat{\mathbf{U}}$, becomes

$$\hat{\mathbf{U}} = \arg\max_{\sigma^2_{\vec{e}}}\left\{\mu_{\vec{e}} = \frac{1}{N_p}\sum_{k=0}^{N_p-1} e[k], \sigma^2_{\vec{e}} = \frac{1}{N_p}\sum_{k=0}^{N_p-1}(e[k] - \mu_{\vec{e}})^2\right\}$$

Based on the assumption from Equation (12)

$$= \arg\max_{\sigma^2_{\vec{q}}}\left\{\mu_q = \frac{1}{N_p}\sum_{k=0}^{N_p-1} e[k], \sigma^2_q = \frac{1}{N_p}\sum_{k=0}^{N_p-1}(e[k] - \mu_q)^2\right\} \tag{13}$$

Equation (13), together with the uncertainty due to having only N_p samples, implies that the optimum threshold for the energy detector is

$$\gamma = \sigma^2_w + \alpha\sigma^2_q \tag{14}$$

where σ^2_w denotes the power of random process w given in Equation (3) and $0 < \alpha < 1$. Note that the optimal value of α could be considered to be the function of reliability or certainty level of the estimation along with the transient model. α could also be regarded as the parameter that captures the particular statistical behavior of the disturbance.

3. Proposed Energy Detector Approach

Faults and/or anomalies presumably present in a natural phenomenon could be classified in several ways. For the sake of simplicity, one could visualize that the characteristics of the natural phenomenon of interest could be captured via a 1D signal whose independent variable is time and its dependent variable is amplitude. In such a simple scenario, intuitively, independent-variable-based strategies—namely, the temporal characteristics of anomalies—could be studied first. In this regard, anomalies that occur in short or very short windows could easily be distinguished from the ones that occur in long or very long windows, where the discrimination between a short and long window is determined by the nature of the phenomenon of interest.

Another way of classifying the anomalies present in a natural phenomenon is, of course, based on the dependent variable, namely, the amplitude characteristics of the anomalies could be studied as well. For instance, there might exist anomalies that exhibit high amplitude characteristics with respect to a nominal amplitude level, whereas there

might be low amplitude characteristics present relative to the high amplitude regime with respect to, again, the nominal amplitude level.

Evidently, a more sophisticated approach would be the amalgamation of the two aforementioned approaches, which considers both the temporal window and amplitude regime simultaneously. Despite the fact that this sophisticated strategy seems to perform better in localizing the anomaly in a 1D signal, it would suffer from the case that includes two different temporal window categories impinging on each other: a very short window anomaly within a very long window anomaly. A similar problem is also valid for the amplitude domain as well. In order to alleviate such problems, generally, a recursive or nested strategy is adopted. The key point of a recursive strategy is known to be coarse-then-fine-search, which first tries to identify the presence of very long temporal window anomalies and then narrows down to shorter windows gradually. In this manner, even though a single-shot solution is not achieved, at least, a single method is employed back to back in a gradual manner.

Inspired by the reasoning above, in this work, a method (also illustrated in Figure 1) that benefits from a single technique and that could run on the different temporal scales in case is needed. This way, if the characteristics of the anomaly are known a priori, the method directly executes with the most suitable temporal window selection. In case no a priori information is available, the method starts narrowing down the temporal window gradually, employs a check as to whether an anomaly is present within the contemporary window, and proceeds down further.

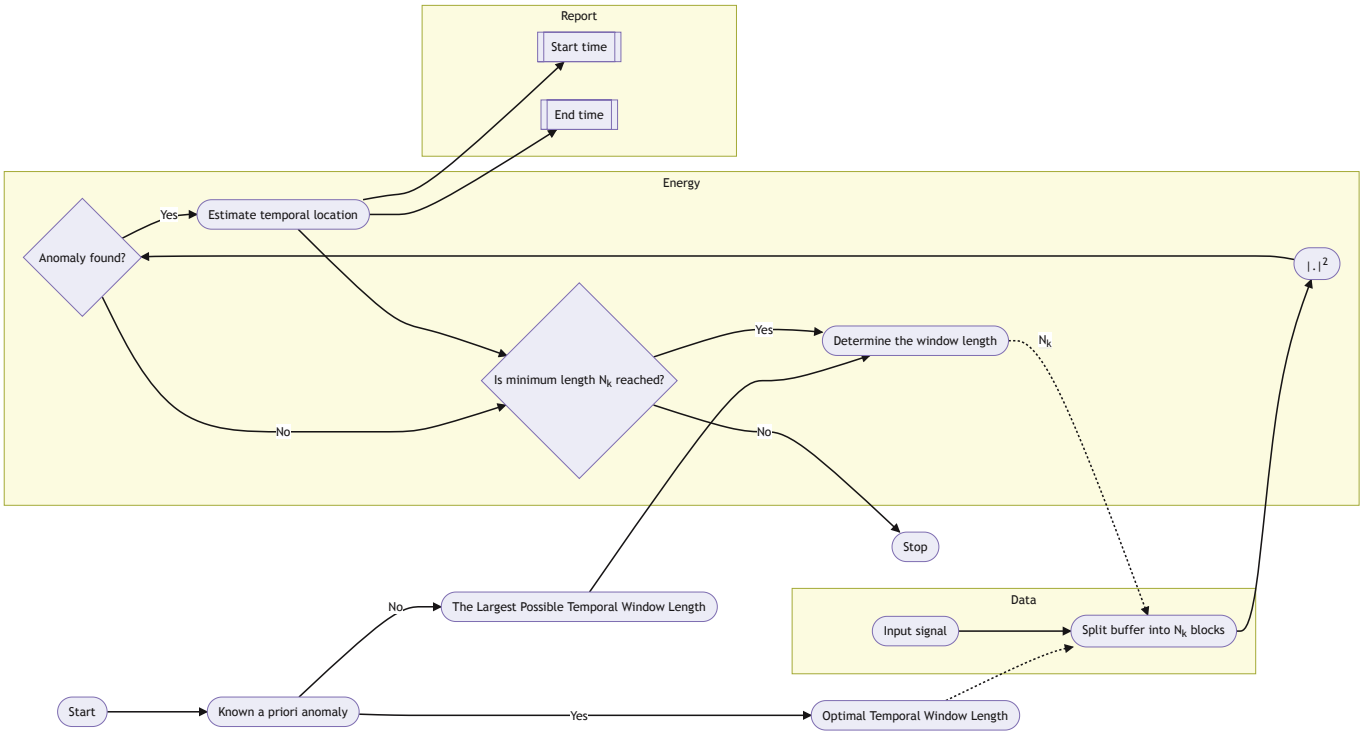

Figure 1. Illustration of the flowchart for the proposed energy detector approach.

4. Case Studies and Results

Power quality failures can be classified under seven sub-categories: transient, short- and long-duration variations, voltage fluctuations, power frequency variations, voltage imbalances, and waveform distortions [18]. In order to align with the descriptions given, we evaluate the performance of our algorithm with existing real-world waveforms in the Grid Signature Library (GSL) data repository [19] and the DOE/EPRI National Database Repository of Power System Event database [20]. The GSL is a framework for smart grid event signatures for the Nation's Energy Sector and Critical Infrastructure. An arcing jumper, a sag fault on a transmission line during a thunderstorm, an impulsive transient

due to lightning, line capacitor switching, recloser blocked, and fast switching transient events are downloaded in "*csv*" format from [19]. The disturbance event number "21831" is selected from the DOE/EPRI National Database Repository of Power System Event database, which corresponds to transformer failure due to lightning [20]. MATLAB 2021B is used to run the algorithm for detection of the aforementioned waveforms on a laptop with an Intel i7-8665U CPU @ 1.9 GHz and 32 GB RAM.

In general, as shown in Figure 2, the proposed low-complexity energy detector algorithm detects all the anomalies. However, each type of anomaly manifests distinct characteristics. The proposed detector could capture them with the help of the $p_{T_q}[n]$ concept given in Equation (3). For instance, Figure 2a depicts the detection performance for an arcing event whose most striking characteristic is its duration, which is longer compared with those of the other anomalies. In Figure 2b, on the other hand, relatively low PAPR change happens to take place in a considerably short period of time (implying a different $p_{T_q}[\cdot]$ configuration) compared with that in Figure 2a; however, the proposed algorithm could still successfully identify the presence of the anomaly with precise start and end times.

In Figure 2c, a different amalgamation of the characteristics present in Figure 2a,b is observed: dramatic change in PAPR (PAPR is defined as the peak signal power inside one observation frame, normalized to the average signal power. It is one of the most effective parameters in estimating the long-term statistical changes.) observed in a very short period of time. Nevertheless, the proposed algorithm acquires the temporal region of anomaly well. In Figure 2d, the importance of the parameter α is apparent. A sub-optimal selection of α manages to capture the start time of the anomaly; however, during fading of the anomaly, which coincidentally overlaps the bending point of the trough of the fundamental frequency, as defined in Equation (1), the proposed detector is unable to detect the precise ending time. The effect of optimal selection of α in accordance with Equation (13) and Equation (14) is seen in Figure 2e. Anomalies that have both relatively longer and shorter times taking place on both the positive-slope region and on and around the crest, respectively, are both successfully detected by the proposed algorithm. Finally, Figure 2f presents the performance of the proposed algorithm for both strong and impulsive nature transients. As expected, the energy detector performs satisfactorily against transient events with high SNR. Similar to Figure 2f, we also utilized the publicly available DOE/EPRI National Database Repository of Power System Event database [20]. It is shown in Figure 3 that the proposed algorithm precisely detects the anomaly region for strong and impulsive nature transients. We provide the detection performance for both current and voltage waveforms.

In order to provide better interpretation of the performance results shown in Figures 2 and 3, we construct Table 2. The energy detector error margin for estimation of the correct start and end times of the anomaly region in terms of sample size lies between 0 and 52 samples. Please note that this corresponds to a 0.00337989 s estimation error for the given waveform as the worst case scenario. For instance, the EPRI 21831 event has 30,721 samples for both current and voltage waveforms. The time difference for the starting point of the actual anomaly is -0.001039966 and the time difference for the end of the actual anomaly is -0.00337989. Note that both performance metrics can be positive or negative, indicating an early or late detection.

Table 2. Performance results of the proposed energy detector with respect to the reference data provided from the Grid Signature Library [19] and EPRI/DOE [20].

Sig ID	# Total Sample per Waveform	Duration of Waveform (in Sec.)	Time per Sample (in Sec.)	Reference Start Sample	Estimated Start Sample	Reference End Sample	Estimated End Sample	# Sample Difference for Start	# Sample Difference for End	Time Difference for Start (in Sec.)	Time Difference for End (in Sec.)
Arcing Jumper under t7577	30,721	1.9968	6.49979E-05	5921	5957	10,129	10,100	36	−29	0.002339924	−0.001884939
A fault on Transmission Line during a thunderstorm caused a SARFI 70 sag	1280	0.16658	0.000130141	296	298	958	955	2	−3	0.000260281	−0.000390422
Lightning cause	1152	0.149928	0.000130146	242	244	262	259	2	−3	0.000260292	−0.000390438
Line capacitor switching	168,960	11	6.51042E-05	30,714	30,715	30,750	30,738	1	−12	6.51042E-05	−0.00078125
Phase C of a multi-phase fault that blows fuse or trips recloser with reclosing blocked	199,680	13	6.51042E-05	30,852	30,862	30,876	30,871	10	−5	0.000651042	−0.000325521
Fast transient due to the switching event	3397	0.17	5.00442E-05	1360	1367	1463	1442	7	−21	0.000350309	−0.001050927
EPRI 21831 Transformer died under t3309 (VoltagePhaseC)	30,721	1.9968	6.49979E-05	11,742	11,742	11,906	11,901	0	−5	0	−0.000324989
EPRI 21831 Transformer died under t3309 (CurrentPhaseC)	30,721	1.9968	6.49979E-05	11,742	11,726	11,906	11,854	−16	−52	−0.001039966	−0.00337989

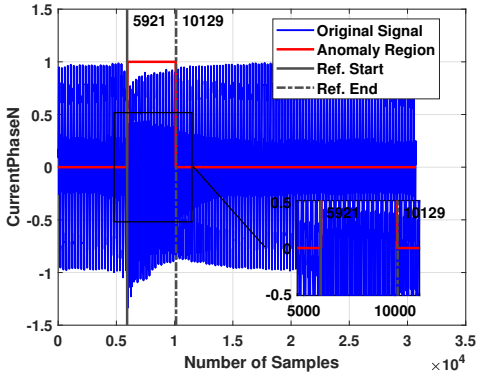

(**a**) Arcing jumper under t7577.

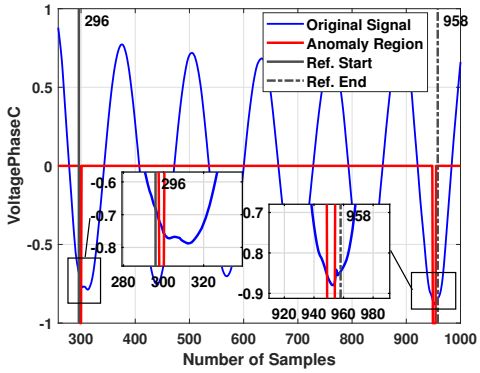

(**b**) A fault on Transmission Line during a thunderstorm caused a SARFI 70 sag.

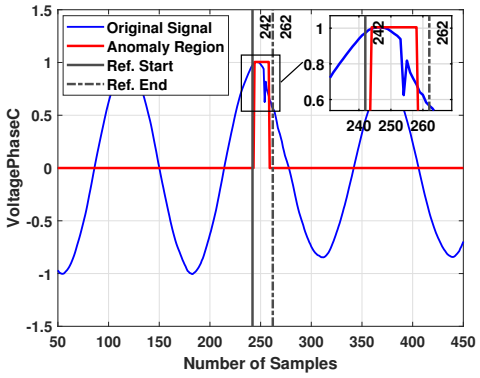

(**c**) Lightning cause.

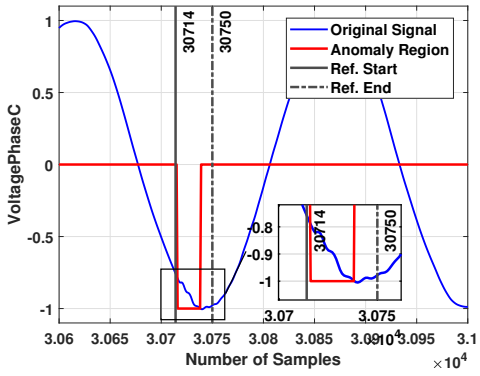

(**d**) Line capacitor switching.

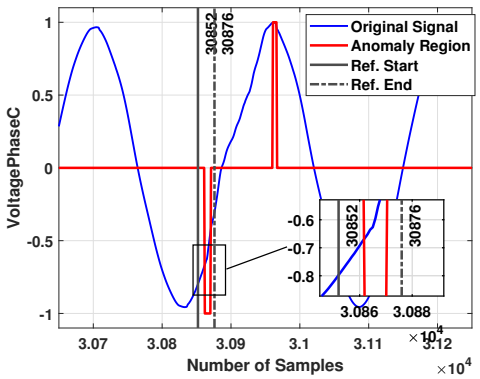

(**e**) Phase C of a multi-phase fault that blows fuse or trips recloser with reclosing blocked.

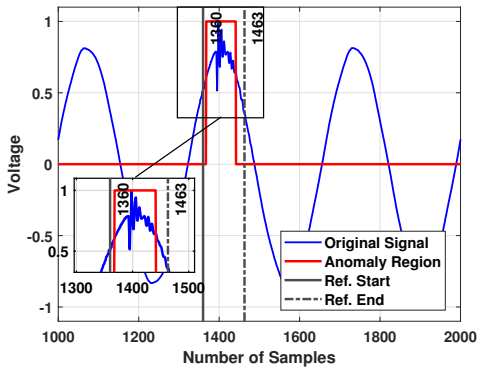

(**f**) Fast transient due to the switching event.

Figure 2. Detection performance of the proposed energy detector approach for Grid Signature Library waveforms [19]. Red lines show the output of the algorithm, and blue lines represent the original captured waveform. Black lines show the reference anomaly start sample and end sample, respectively.

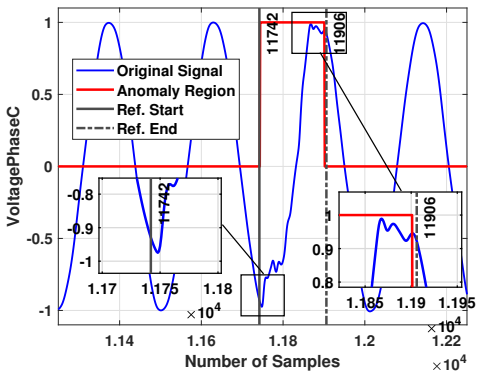

(**a**) EPRI 21831—Transformer died under t3309.

(**b**) EPRI 21831—Transformer died under t3309.

Figure 3. Detection performance of the proposed energy detector approach for DOE/EPRI National Disturbance Library [20]. Red lines show the output of the algorithm, and blue lines represent the original captured waveform. Black lines show the reference anomaly start sample and end sample, respectively.

5. Runtime Analysis

With a buffer length of N, the method requires N squaring operations followed by $N-1$ summations. Squaring can be implemented efficiently using the Toom–Cook or Karatsuba methods, reducing complexity from $O(n^2)$ to $\approxeq O(n^{1.465})$. The proposed method is, therefore, of $O(n)$ spatial complexity and $O(n^p)$ computational complexity, where $p < 1.585$. This implies that increasing the buffer size (N in Equation (6)) will definitely improve the estimation accuracy, while not affecting the computational complexity. Therefore, spatial complexity of $O(n)$ is an important design parameter for physical implementation of the proposed algorithm. On the other hand, the proposed algorithm has computational complexity of $O(n^p)$, where $p < 1.585$, which is not affected by the spatial complexity.

6. Concluding Remarks and Future Directions

This study investigates the detection of existing real-world transient waveforms such as arcing, impulsive, and sag events in grid infrastructure by employing a low-complexity energy detector algorithm. The results are satisfactory in terms of anomaly detection. With the increasing demand for the deployment of low-cost and low-battery-consuming Internet of Things (IoT) devices on the edge, the proposed algorithm can be easily embedded onto existing sensors due to its simple design and low complexity. In the future, we will explore implementing the algorithm onto the devices for real-time monitoring.

Author Contributions: Conceptualization, A.R.E., A.W., S.Y. and P.F.; methodology, A.R.E., A.W., S.Y. and P.F.; validation, A.R.E.; formal analysis, A.R.E., A.W. and S.Y.; investigation, A.R.E., A.W. and S.Y.; resources, A.R.E., A.W. and S.Y.; data curation, A.R.E., A.W. and J.O.; writing-original draft preparation, A.R.E.; writing-review and editing, A.R.E., A.W., J.O., J.H.II, S.Y. and P.F. All authors have read and agreed to the submitted version of the manuscript.

Funding: This research received funding from US Department of Energy (DOE).

Institutional Review Board Statement: Not applicable.

Informed Consent Statement: Not applicable.

Data Availability Statement: Not applicable.

Conflicts of Interest: The authors declare no conflicts of interest.

Abbreviations

ADC	analog-to-digital converter
DWT	discrete wavelet transform
GSL	Grid Signature Library
IoT	Internet of Things
MLE	maximum likelihood estimation
PAPR	peak-to-average power ratio
PDF	probability density function
RMS	root mean square
ROC	receiver operating characteristic
SNR	signal-to-noise ratio
SINR	signal-to-interference-plus-noise ratio
STFT	short-time Fourier transform

References

1. Alonso, M.; Amaris, H.; Alcala, D.; Florez R., D.M. Smart Sensors for Smart Grid Reliability. *Sensors* **2020**, *20*, 2187. [CrossRef] [PubMed]
2. Minh, Q.N.; Nguyen, V.H.; Quy, V.K.; Ngoc, L.A.; Chehri, A.; Jeon, G. Edge Computing for IoT-Enabled Smart Grid: The Future of Energy. *Energies* **2022**, *15*, 6140. [CrossRef]
3. Rivas, A.E.L.; Abrao, T. Faults in Smart Grid Systems: Monitoring, Detection and Classification. *Elsevier Electric Power Syst. Res.* **2020**, *189*, 1–26.
4. Mahmoud, M.A.; Md Nasir, N.R.; Gurunathan, M.; Raj, P.; Mostafa, S.A. The Current State of the Art in Research on Predictive Maintenance in Smart Grid Distribution Network: Fault's Types, Causes, and Prediction Methods—A Systematic Review. *Energies* **2021**, *14*, 5078. [CrossRef]
5. California Department of Forestry and Fire Protection (CAL FIRE). 2020 Wildfire Activity Statistics. Available online: https://www.fire.ca.gov/media/0fdfj2h1/2020_redbook_final.pdf (accessed on 18 March 2022).
6. Farooq, U.; Bass, R.B. Frequency Event Detection and Mitigation in Power Systems: A Systematic Literature Review. *IEEE Access* **2022**, *10*, 61494–61519. [CrossRef]
7. Senaratne, D.; Kim, J.; Cotilla-Sanchez, E. Spatio-Temporal Frequency Domain Analysis of PMU Data for Unsupervised Event Detection. In Proceedings of the IEEE ISGT Power & Energy Society Innovative Smart Grid Technologies Conference, Washington, DC, USA, 16–18 February 2021; pp. 1–5.
8. Ma, D.; Hu, X.; Zhang, H.; Sun, Q.; Xie, X. A Hierarchical Event Detection Method Based on Spectral Theory of Multidimensional Matrix for Power System. *IEEE Trans. Syst. Man. Cybern. Syst.* **2021**, *51*, 2173–2186. [CrossRef]
9. Niu, H.; Omitaomu, O.A.; Cao, Q.C. Machine Committee Framework for Power Grid Disturbances Analysis Using Synchrophasors Data. *Smart Cities* **2021**, *4*, 1–16. [CrossRef]
10. Khoa, N.M.; Dai, L.V. Detection and Classification of Power Quality Disturbances in Power System Using Modified-Combination between the Stockwell Transform and Decision Tree Methods. *Energies* **2020**, *13*, 3623. [CrossRef]
11. Follum, J.; Holzer, J.; Etingov, P. A Statistics–based Threshold for the RMS–energy Oscillation Detector. *Int. J. Electr. Power Energy Syst.* **2021**, *128*, 106685. [CrossRef]
12. Zhan, L.; Xiao, B.; Li, F.; Yin, H.; Yao, W.; Li, Z.; Liu, Y. Fault—Tolerant Grid Frequency Measurement Algorithm During Transients. *IET Energy Syst. Integr.* **2020**, *2*, 173–178. [CrossRef]
13. Sun, H.; Li, F.; Sticht, C.; Mukherjee, S. Circular Trajectory Approach for Online Sinusoidal Signal Distortion Monitoring and Visualization. *IEEE Trans. Smart Grid* **2022**, *4*, 3315–3318. [CrossRef]
14. Vasile, C.; Ioana, C. On the Multi-modal Sensing of Electrical Arcs. In Proceedings of the IEEE SAS Sensors Applications Symposium, Glassboro, NJ, USA, 13–15 March 2017; pp. 1–5.
15. Sousa, M. Limitations of Crosscorrelation Radiometer Performance. In Proceedings of the IEEE MILCOM Military Communications Conference, San Diego, CA, USA, 11–14 October 1992; pp. 816–821.
16. Urkowitz, H. Energy Detection of Unknown Deterministic Signals. *Proc. IEEE* **1967**, *55*, 523–531. [CrossRef]
17. Digham, F.F.; Alouini, M.S.; Simon, M.K. On the Energy Detection of Unknown Signals Over Fading Channels. *IEEE Trans. Commun.* **2007**, *5*, 3575–3579. [CrossRef]
18. Transmission & Distribution Committee Power Quality Subcommittee Working Group on Power Quality Data Analytics. Electric Signatures of Power Equipment Failures: IEEE PES–TR73. Available online: https://resourcecenter.ieee-pes.org/publications/technical-reports/PES_TP_TR73_TD_122019.html (accessed on 18 April 2022).
19. Oak Ridge National Laboratory and Lawrence Livermore National Laboratory. Grid Signature Library. Available online: https://gsl.ornl.gov/ (accessed on 8 August 2022).
20. DOE/EPRI National Database Repository of Power System Events. Available online: https://pqmon.epri.com/see_all.html (accessed on 19 October 2022).